Water SA 52(2) 161–173 / Apr 2026
https://doi.org/10.17159/wsa/2026.v52.i2.4175

Research paper

Nanofiltration membranes for high-efficiency separation of microplastics from wastewater

Michela Masango[1,3,4], Gokul Sreekumar[2], Praveen Keerthi[2], Nonhlangabezo Mabuba[1,3] and Soraya P Malinga[1,4]

[1]*Department of Chemical Sciences, University of Johannesburg, Doornfontein Campus, P.O. Box 17011, Doornfontein, Johannesburg, 2028, South Africa*
[2]*Department of Chemistry, Anna University, Sardar Pa Road, Guindy Chennai, Chennai Tamil Nadu 600025, India*
[3]*Centre for Nanomaterials Science Research, University of Johannesburg, South Africa*
[4]*Joint Research Centre for Water, Environmental Science Technology, University of Johannesburg, South Africa*

This study investigated the occurrence and removal of microplastics (MP) in samples collected from the influent and effluent of a municipal wastewater treatment plant and from specific stages of an industrial water treatment plant, including the raw water, clarifier, sand filter, and mixed bed outlet. The wet-peroxide oxidation method was used to isolate the microplastics, and these were characterised by techniques such as stereomicroscopy, scanning electron microscopy (SEM), and attenuated total reflectance–Fourier transform infrared spectroscopy (ATR–FTIR) to determine properties such as shape, colour, size and polymer composition. Hyperbranched polyethyleneimine (HPEI) polyethersulfone (PES) thin-film composite membrane prepared via interfacial polymerisation was used to reject the isolated microplastics. Nylon-6 and polyethylene were found to be the most predominant polymers, which were either blue, black or red in colour. The most common shapes in both sampling areas were primarily fibres (48.5%), fragments (30.3%), and films (21.2%) and the presence of such morphologies was influenced by various anthropogenic activities. Whilst the microplastic abundance ranged from 2.22 ± 1.11 MP/L to 24.44 ± 11.50 MP/L. The membranes achieved a rejection efficiency of 97.33% through size exclusion and hydrophilic–hydrophobic interactions. These findings demonstrate the prevalence of microplastics in both influent and effluent and highlight the potential for HPEI/PES nanofiltration membrane technology as a viable and scalable technology for the rejection of microplastics in wastewater.

CORRESPONDENCE
Soraya P Malinga

EMAIL
smalinga@uj.ac.za

DATES
Received: 17 October 2024
Accepted: 2 April 2026

KEYWORDS
hyperbranched polyethyleneimine
microplastics
nanofiltration membrane
polyethersulfone
municipal wastewater treatment plant

INTRODUCTION

Plastic pollution in the environment is a growing concern worldwide. According to Ma et al. (2019a), plastic residues are often transported over long distances by hydrodynamic processes and through mechanical action, and they gradually degrade over time. During these degradation processes, tiny particles smaller than 5 mm are formed, commonly referred to as microplastics (Ma et al., 2019a). Microplastics can be categorised into two types, i.e., primary and secondary microplastics (Hidayaturrahman and Lee, 2019; Zheng et al., 2023). Primary microplastics are intentionally manufactured and examples include microbeads and plastic powder used in personal care products and in moulding pellets and scrubbers, respectively (Horton et al., 2018). Secondary microplastics result from the breakdown of larger plastics and are triggered by processes such as ultraviolet radiation and physical stress (Zheng et al., 2023).

The reduction of microplastic pollution in the environment has become an urgent matter. This is because microplastics act as carriers of pollutants as they tend to absorb toxic chemicals such as pharmaceuticals, pesticides and toxic metals (Zn, Cu, Pd, and Ag) due to their large surface area and hydrophobic nature (Ma et al., 2019a; Ma et al., 2019b). Once ingested, these contaminated microplastics can cause diseases such as cancer, reduced immune response and reduced reproductivity in animals and humans (Nouri et al., 2025). In South Africa, approximately 72% of plastic packaging is not recovered, as 40% is disposed of in landfills while the remaining 32% leaks out from collection systems and is illegally dumped (Bonthuys, 2018). Wastewater treatment plants (WWTPs) were not designed to fully retain microplastics, as many studies have found that microplastics with a size smaller than 20 μm are not retained and are subsequently released into the environment (Poerio et al., 2024). Thus, the increasing presence of microplastics in water bodies has intensified the need to investigate effective wastewater treatment regimes. Methods such as incineration, landfills, thermal degradation and biodegradation have been used to eradicate microplastics from the environment, but these are costly as they require high temperatures (up to 400°°C) and complex catalysts, thus limiting their practicality (Russo et al., 2025). Membrane technology is a promising solution that can be scaled up and integrated with other existing technologies, resulting in a high retention of microplastics coupled with low cost implications (Russo et al., 2025). Dey et al. (2021) demonstrated the potential of membrane technology in the separation of microplastics from wastewater but highlighted the need for preparing membranes with enhanced surface properties that will enhance hydrophilic–hydrophobic and electrostatic repulsion between negatively charged microplastics and the membrane surface. To impart such properties, hyperbranched polyethyleneimine polymer was used as an additive in the preparation of thin-film composite (TFC) membranes. Hyperbranched

polyethyleneimine (HPEI) is a branched macromolecule that has dense hydrophilic functional groups (-NH_2), with numerous internal cavities and has superior compatibility with most polymers. These hyperbranched polymers have been found to induce several properties in membranes, such as hydrophilicity, charge separation, adjustment of membrane pores, and inner and outer voids. These properties increase water permeability whilst providing steric hindrance to ions and molecules, thus enhancing pollutant rejection (Zhang et al., 2024).

Specifically, this work assesses the qualitative analysis of microplastics present in influent and effluent collected from a municipal wastewater treatment plant and an industrial water treatment plant. Furthermore, the effectiveness of the hyperbranched polyethyleneimine polyethersulfone (HPEI/PES) nanofiltration membrane towards the removal of microplastics also underlines the importance of integrating this technology in existing plants.

METHODOLOGY

Material

Ferrous sulphate heptahydrate ($FeSO_4{\cdot}7H_2O$, 99.5%), hydrogen peroxide (H_2O_2, 30%), and sodium chloride (NaCl) were purchased from Sigma-Aldrich, South Africa.

Sampling site, operations and collection

Samples were collected at two industrial water treatment plants (labelled Plants A and B) located in Mpumalanga. The first industrial water treatment plant, Plant A, abstracts its raw water from the Usutu River, which is influenced by textile industries, sugar mills, urban settlements, and surrounding vegetation. The second industrial water treatment plant, Plant B, abstracts its raw water from the Vaal River, which is impacted by coal mining, industrial discharges, agricultural activities, and nearby rural and urban settlements (Juizo and Hjorth, 2009; Wepener et al., 2011). The industrial water treatment plants, Plants A and B, treat raw water for production purposes using a conventional multi-stage approach illustrated in Fig. 1. The water passes through key water treatment stages: the raw water, clarifiers (sedimentation of suspended solids), sand filters (removal of fine particulates), and mixed beds (cation and anion exchange resins for polishing and ion removal). Samples were collected from each of these stages to assess the presence of microplastics and removal efficiency across the treatment train.

The municipal wastewater treatment plant, Plant C, is located in Gauteng. It receives influent from diverse sources, including residential properties, lodging facilities, shopping centres, and commercial buildings, which gives a composition of 90% domestic wastewater and only 10% industrial wastewater (Muller et al., 2004). The treatment process (Fig. 2) follows a conventional wastewater management sequence comprising screening (removal of coarse solids and debris), preliminary sedimentation (settling of suspended solids), biological treatment through trickling filters (organic matter degradation via microbial activity), and secondary clarification (separation of treated effluent from biomass). The effluent is discharged into a receiving river. For this study, samples were collected only from the influent and the effluent, providing an overview of the plant's overall performance in removing microplastics.

All samples were collected in pre-cleaned amber bottles (washed with nitric acid), rinsed with sampling wastewater before collection and immediately stored in portable ice chests with ice. Samples were transported to the laboratory and stored at 4°C until analysis. The raw water points for both industrial water treatment plants, Plants A and B, are illustrated in Fig. 3, as well as the location of the municipal wastewater treatment plant, Plant C.

Sample pre-treatment method

The wet peroxide oxidation method (Fig. 4) was employed to oxidise any natural organic matter present in the sample and to isolate microplastics from the collected samples. A Fenton reagent, prepared by combining ferrous sulphate heptahydrate ($FeSO_4{\cdot}7H_2O$, 99.5%) with hydrogen peroxide (H_2O_2), was

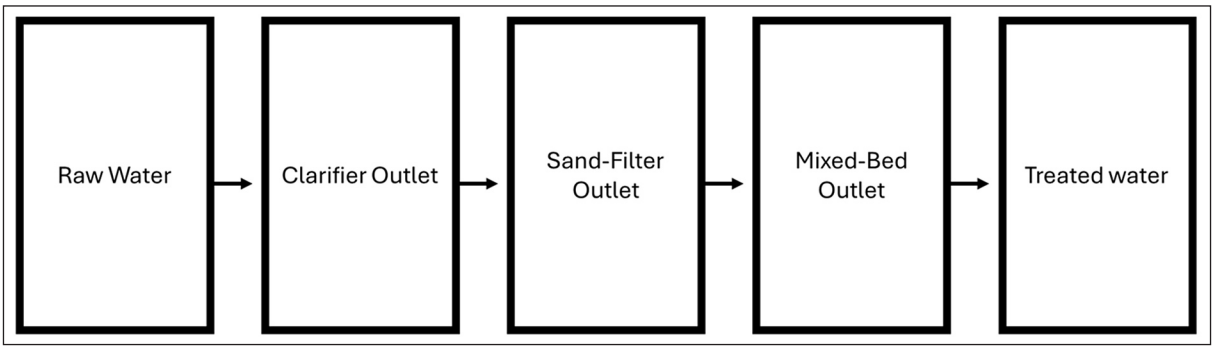

Figure 1. Flow diagram showing the operations and the water treatment pathway for samples collected from the industrial water treatment plants, Plants A and B

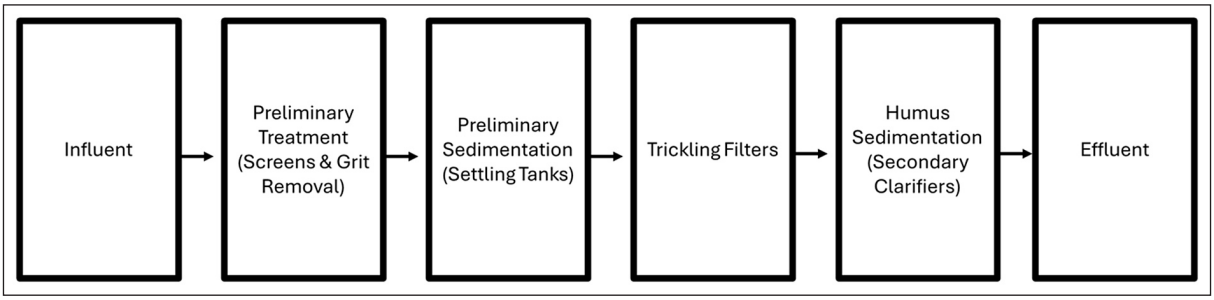

Figure 2. Simplified flow diagram showing the treatment stages in the municipal wastewater treatment plant (Plant C)

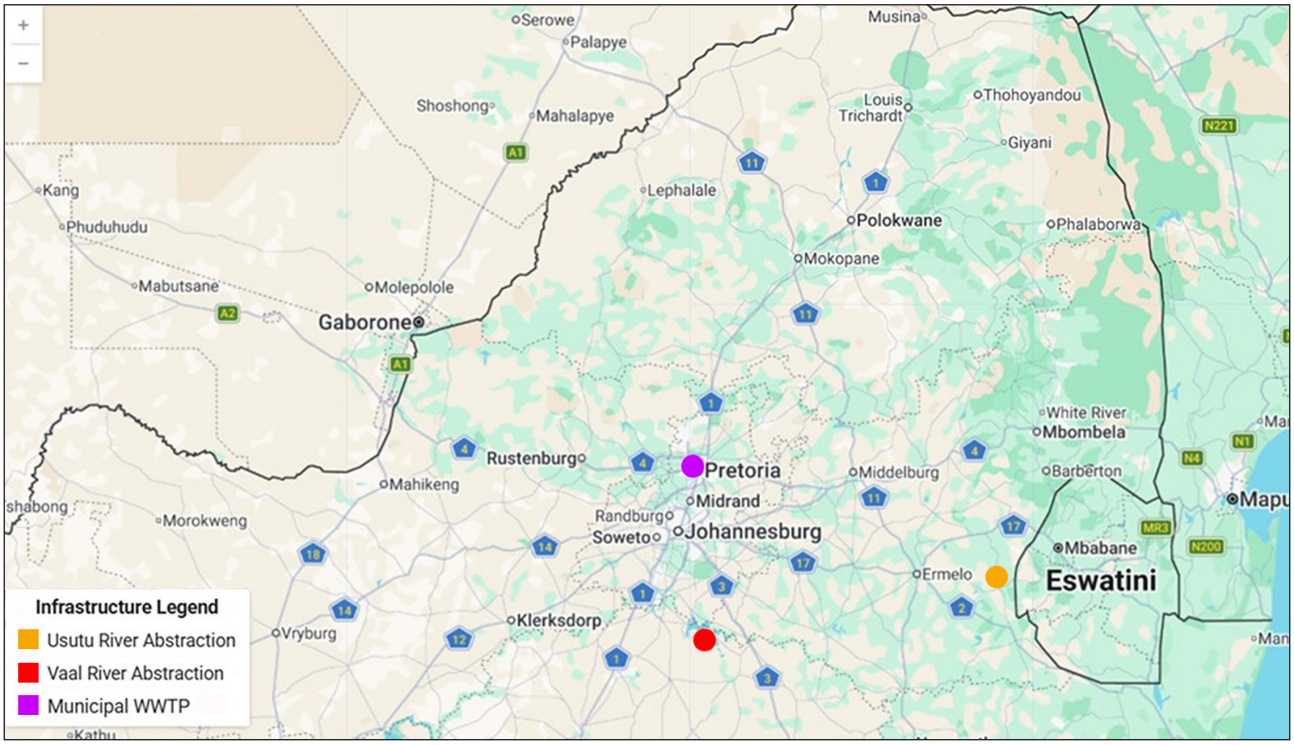

Figure 3. River abstraction points for industrial water treatment plants, Plants A and B; location of the municipal wastewater treatment plant, Plant C

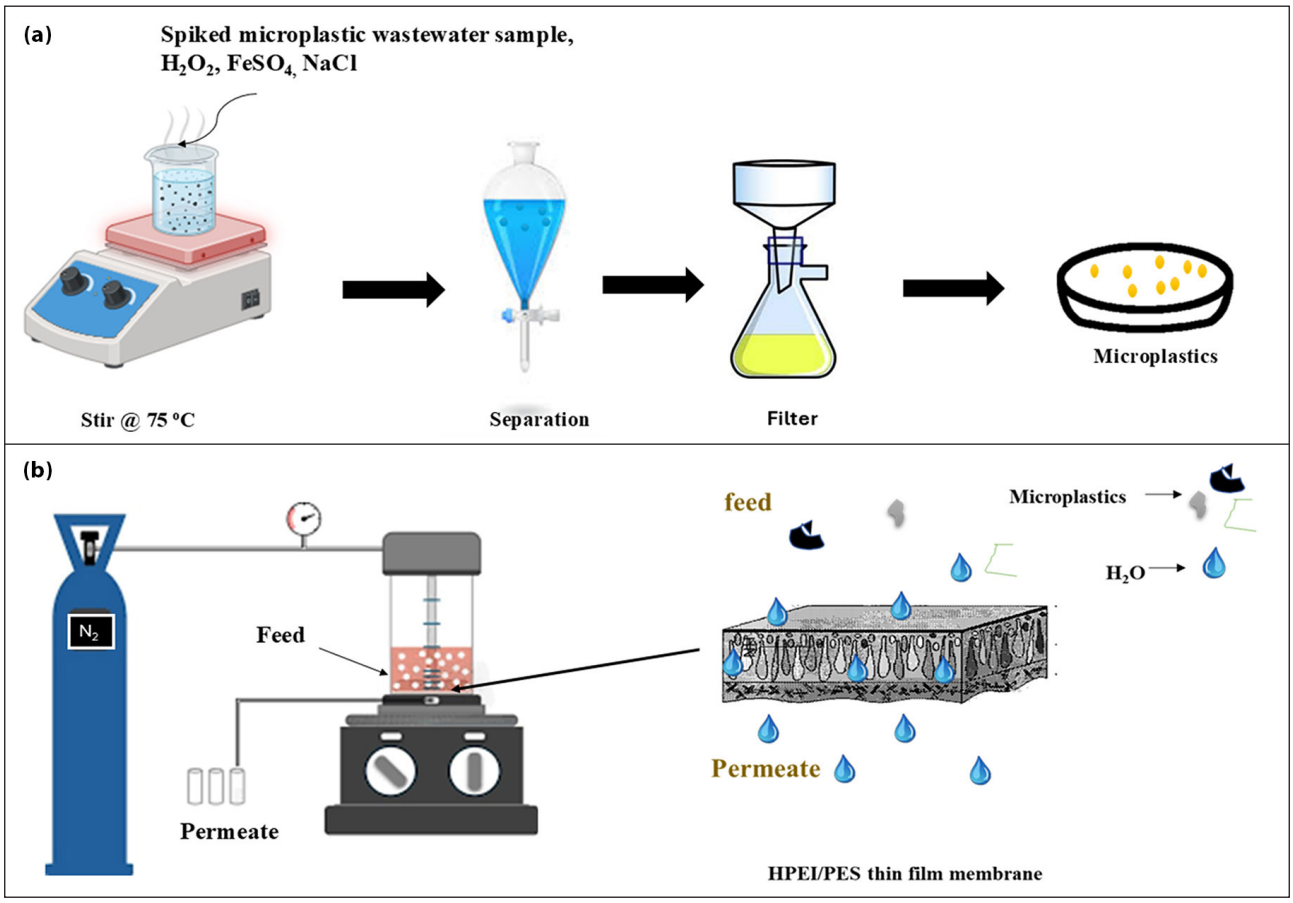

Figure 4. Schematic diagram illustrating the (A) extraction and (B) removal of the microplastics using the prepared membranes

added to each sample (450 mL) and allowed to stand for 5 min at room temperature. This mixture was then heated to 75°C under continuous stirring for 30 min. Subsequently, sodium chloride (6 g) was added to increase the solution density. Heating was continued until complete dissolution of the salt was observed, after which the solution was transferred into a separating funnel and left to settle overnight. The solution was filtered using Whatman filter paper (pore size of 2.5 µm) to remove residual organic matter. The retained material was then oven-dried at 60°C for 24 h (Nkosi et al., 2022).

Preparation of HPEI/PES thin-film composite membranes and removal of microplastics

The HPEI/PES thin-film composite membranes were prepared via interfacial polymerisation (see Appendix, Tables A1 and A2) following the procedures described in our previous study, Vlotman et al. (2018). Figure 4 presents a schematic diagram summarising the extraction of microplastics and their subsequent removal using the HPEI/PES membrane. Initially, a pre-treatment method known as wet peroxide oxidation was employed to extract the microplastics from the wastewater samples. Following the extraction, the isolated microplastics were used to prepare a spiked wastewater sample, which served to assess the performance of the HPEI/PES membrane in removing microplastics.

Quality control

Fume hoods were used for quality control and to minimise airborne contamination of the samples. Routine cleaning and maintenance of the laboratory and fume hoods helped maintain a low contamination profile. Lab coats were worn to restrict the shredding of fibres from clothing. As an extra precaution, blue latex gloves were used for handling microplastic samples; blue gloves were specifically chosen for their distinct colour, which rendered contamination easier to spot. Metal and glass materials were preferred for handling, as plastics can release particles (Prata et al., 2021). Amber glass bottles were used for sample storage and to prevent contamination from occurring.

Instrumentation

Characterisation techniques

Microplastic particles were identified using a stereomicroscope (Zeiss, SteREO discovery microscope) equipped with an AxioCam HRC digital camera, providing 1 000 µm resolution and 4.5× magnification. This microscope was used to digitise, photograph, and count the microplastics. The length of the microplastics was measured using ImageJ software (Zhang et al., 2018). To obtain the spectral profile of the pre-identified particles, the microplastics were analysed using attenuated total reflectance–Fourier transform infrared spectroscopy (ATR–FTIR), using an instrument acquired from Perkin Elmer, Johannesburg. Spectrum 10 spectroscopy was used to determine the exact composition of the microplastics. The surface morphology of the microplastics was examined using a Vega3 SEM series at a working distance of 200 µm, and samples were carbon-coated before analysis. The DataPhysics Optical Contact Angle equipped with a camera was used to measure the hydrophilicity of the prepared membrane. Ten drops of deionised water were placed at different positions on the membrane surface to obtain the mean contact angle.

The water uptake measurements were determined by immersing the membranes in deionised water for 24 h. The mass difference of the membrane between dry and wet was used to determine the water uptake capacity, and was calculated using Eq. 1 (Athira et al. 2020):

$$\text{Water uptake } \% = \frac{W_W - W_d}{\text{W}_\text{d}} \times 100 \quad (1)$$

where: W_w is the weight of the wet membrane, and W_d is the weight of the dry membrane. The porosity (ε%) of the membrane was calculated using Eq. 2 (Letswalo et al., 2022):

$$(\%)\varepsilon = \frac{W_W - W_d}{A \cdot l \cdot d_w} \times 100 \quad (2)$$

where: W_w is the weight of the wet membrane, W_d is the weight of the dry membrane, A is the effective area of the membrane (1 cm^2), l is the thickness of the membrane obtained using ImageJ, and d_w is the density of deionised water (1 g/cm^3 at 25°C).

The mean pore radius (r_m) was calculated using the Guerout-Elfrord-Ferry Equation, Eq. 3, to determine the pore size of the synthesised membranes (Liao et al., 2012).

$$r_m = \sqrt{\frac{(2.9 - 1.75\varepsilon \times 8\eta l Q)}{\varepsilon \text{ x A x } \Delta P}} \quad (3)$$

where: η is the water's viscosity (8.9 × 10^{-4} Pa·s), l is the membrane thickness (m), Q is the volume of pure water passing through the membrane per unit time (m^3/s), ε is the porosity, A is the effective area of the membrane (m^2) and ΔP is the operating pressure (400 kPa).

Membrane rejection studies

A dead-end filtration cell (Sterlitech stirred cell, HP4750) was used to evaluate the rejection of microplastics using the membrane. Filtration experiments were performed using 300 mL of wastewater sample collected from the municipal wastewater treatment plant (Plant C). Filtration was conducted at room temperature, with a transmembrane pressure of 400 kPa using a feed pH of 7 over 180 min. Microplastic rejection (%R) was determined using Eq. 4.

$$\%R = (1 - \frac{C_{\text{perm}}}{C_{\text{feed}}}) \times 100 \quad (4)$$

where: $\%R$ is the percentage rejection, C_{perm} and C_{feed} are the microplastic concentrations in the permeate and feed solution (MP/L), respectively (Enfrin et al., 2020). The amount of microplastics was quantified using a unit of MP/L; microplastics were calculated by dividing the total number of MPs in each sample by the corresponding volume (Bernard et al., 2025).

Characterisation of microplastics

Stereomicroscope qualitative and quantitative analysis of microplastics extracted from the industrial water treatment plants, Plants A and B

Figure 5 (a–f) displays microscope images of samples collected from the raw water, clarifier outlet, sand filter outlet, and mixed bed outlet of Plant A (industrial water treatment plant). Overall, the images reveal numerous fibres, predominantly linear in shape, with an average length ranging from 0.44 ± 1.87 mm to 0.95 ± 0.90 mm. Fibres are derived from fabrics which might originate from the nearby textile industries, rural areas, and urban settlements along the Usutu River, which is the source of the raw water for Plant A (Juizo and Hjorth, 2009). The observed colours included red, blue, black, and yellow. This observation is consistent with previous studies where fibres were found to be the most dominant microplastic type in various aquatic environments (Devriese et al., 2015; Naji et al., 2018; Horton et al., 2018). The microplastic concentrations at the raw water, clarifier outlet, sand filter and the mixed bed outlet were 6.67 ± 2.55 MP/L, 2.22 ± 1.11 MP/L, 0 MP/L, and 8.89 ± 0.66 MP/L, respectively. Concentrations generally decreased along the treatment process train and increased again in the mixed bed outlet. Inspection of the mixed-bed outlet showed elevated microplastic counts, which correspond with the colour and polymer fingerprint of worn resin beads. Although direct reports of microplastic shedding from mixed-bed ion-exchange resins in operational treatment plants are scarce, several studies suggest that polymeric resins under operational load, exposure to particulates or organic matter, and routine chemical exposure can undergo degradation or partial wear. For example, Laforce et al. (2025) observed that anion exchange resins interacting with humic and biopolymeric matter show structural and adsorption stress. Similarly, in a study by Haddad et al. (2019), different resin types under varied water matrices show reduced integrity or increased exhaustion. These findings lend support to the hypothesis that mixed-bed resins can become secondary sources of microplastic particles through mechanical attrition or chemical weakening.

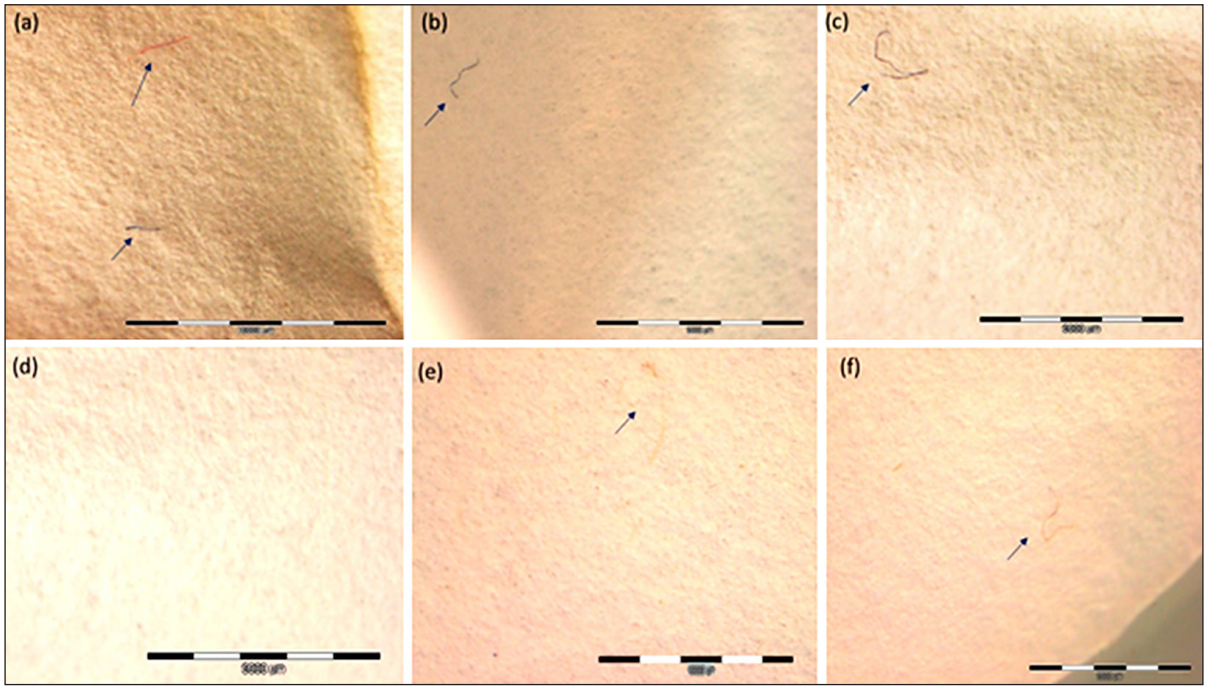

Figure 5. Stereomicroscope images for Plant A (industrial water treatment plant): (a and b) raw water, (c) clarifier outlet, (d) sand filter outlet, and (e and f) mixed bed outlet

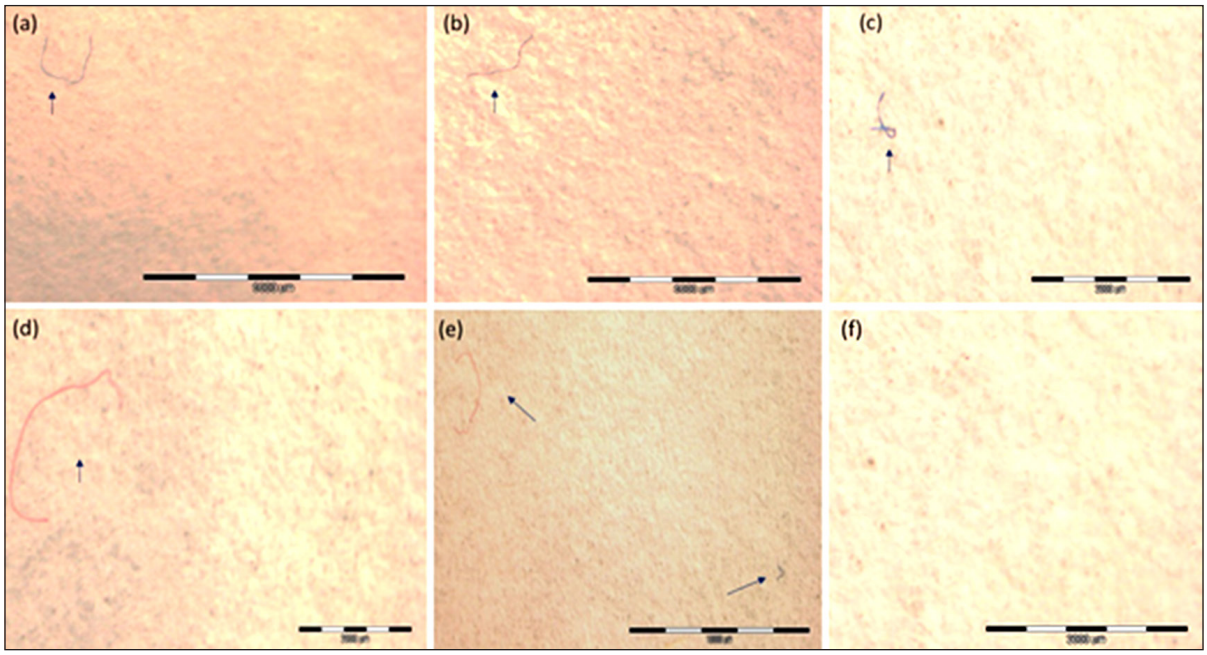

Figure 6. Stereomicroscope images for Plant B (industrial water treatment plant): (a and b) raw water, (c–e) clarifier outlet and (f) mixed bed outlet

Figure 6 (a–e) displays the microplastics observed along the industrial water treatment train for Plant B, which is supplied by the Vaal Barrage. Fibres were detected only in the raw water and clarifier outlet. The fibres observed were predominantly linear in shape and were red, blue and black. The average lengths ranged from 0.98 ± 2.55 to 0.85 ± 0.38 mm. These fibres are mainly attributed to inputs from rural and urban settlements, as well as industrial activities occurring in the vicinity of Vaal Barrage (Gyedu-Ababio and Van Wyk, 2004; Wepener et al., 2011). A reduction in microplastics concentration was observed along the water treatment train, as 3.33 ± 0.90 MP/L, 8.89 ± 7.67 MP/L, 0 MP/L and 0 MP/L were recorded in the raw water, clarifier outlet, sand filter and mixed bed outlet, respectively. These results demonstrate that the sand filter and mixed bed stages were effective in removing microplastics (Wang et al., 2020).

Qualitative and quantitative stereomicroscopy analysis of samples collected from the municipal wastewater treatment plant, Plant C

Figure 7 (a–f) illustrates the morphology of microplastics observed in the influent of the municipal wastewater treatment plant (Plant C). The average length of the detected microplastics was 1.69 ± 0.25 mm, which aligns with the size range reported by Bayo et al. (2020), who observed microplastics from 1–2 mm in urban wastewater streams. Various morphologies were identified, including films, fragments, and fibres, differing in both shape and size. The presence of films is likely attributed to large plastic debris from nearby shopping centres, urban settlements, and commercial buildings, which contribute effluent to the plant (Nkosi et al., 2022; Zhang et al., 2023). Fragments are primarily

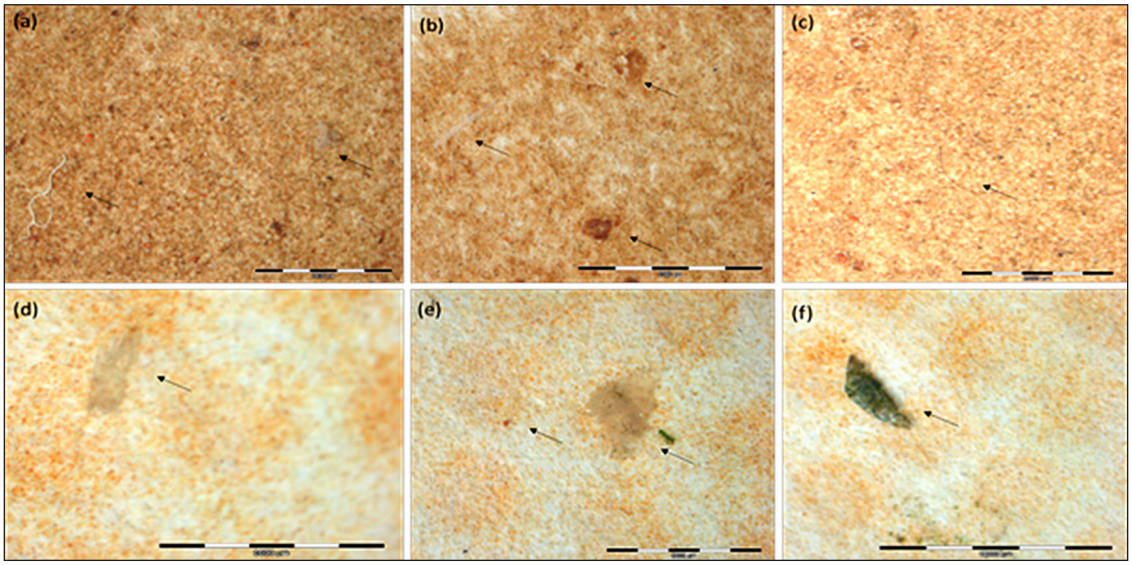

Figure 7. Stereomicroscope images of microplastics observed in the influent of the municipal wastewater treatment plant, Plant C

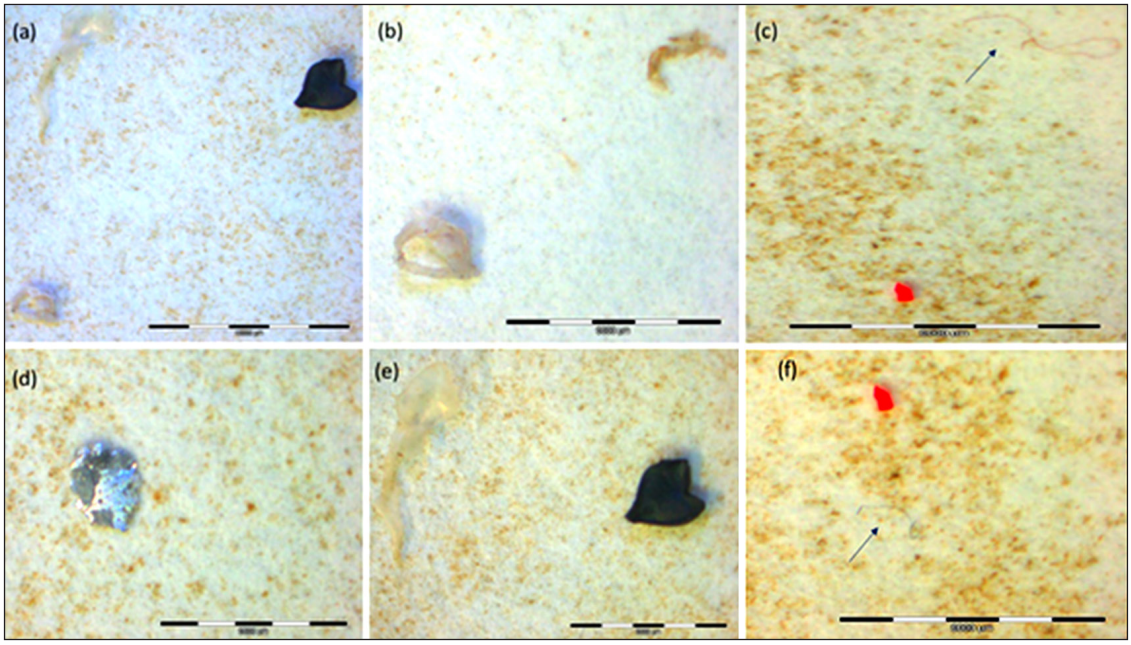

Figure 8. Stereomicroscope images of microplastics in effluent samples collected from municipal wastewater treatment plant, Plant C

derived from the breakdown of packaging materials through mechanical abrasion, UV exposure, and ageing during collection and transport. Fibres, on the other hand, are typically associated with the washing of synthetic textiles, the release of lint from laundry effluents, and domestic wastewater discharge.

The total concentration of microplastics in the effluent was 22.22 ± 0.50 MP/L, which is comparable to findings by Long et al. (2019), who reported concentrations from 2–22.9 MP/L in treated municipal influents in China. The persistence of microplastics in the final effluent, despite conventional treatment, has been attributed to their small size, buoyancy, and poor sedimentation efficiency, allowing them to pass through secondary clarification and biological treatment units. Jiang et al. (2018) also emphasised that micropollutant removal efficiency largely depends on operational parameters such as hydraulic retention time, aeration intensity, and sludge floc formation. Therefore, the observed concentration in this study suggests that similar removal limitations may exist within the investigated plant, particularly in stages where fine particles are not effectively captured or where turbulence resuspends settled microplastics.

Figure 8 (a–f) illustrates the microplastics observed in the effluent of Plant C (municipal wastewater treatment plant). The stereomicroscope images revealed fragments, fibres, and films in various colours, including semi-translucent, red, silver, shiny, and black. In particular, Fig. 8(d) displays a shiny microplastic particle. Such particles are typically composed of metallised polyethylene terephthalate (PET), containing elements such as aluminium, titanium, iron, or bismuth (Blackledge and Jones Jr, 2007). Due to their small size, PET glitters are highly prone to escaping into the environment and are recognised as a significant contributor to microplastic pollution (Fuschi et al., 2022). The potential sources of these microplastics include effluent from shopping centres and urban settlements, while household products often contribute PET through packaging materials (Pilevar et al., 2019). The total concentration of microplastics detected in the effluent was 24.44 ± 11.50 MP/L, with an average particle length of 0.81 ± 0.91 mm. The elevated concentrations in the effluent can be attributed to the recycling of activated sludge, which may contain residual microplastics from the previous treatment cycles (Casella et al., 2025). In wastewater treatment plants, activated sludge is commonly reused to lower

operational costs; however, this practice can compromise effluent quality and lead to increased microplastic levels (Casella et al., 2025).

Table 1 and Fig. 9 present a summary of the shapes, colours, types, and percentage distribution of the extracted microplastics. The analysis indicated that nylon-6 and polyethylene were predominant, with microplastics occurring primarily as fibres (48.5%), fragments (30.3%), and films (21.2%). The dominance of fibre and fragments has been reported to suggest secondary microplastics as the major origin, meaning that these microplastics are fragmented from larger particles of plastic materials (Ilechukwu et al., 2025).

SEM analysis of microplastics

Figure 10 (a–f) presents the morphological characterisation of microplastics using SEM. Figures 10a and 10b show a fibre with an average diameter of 9.50 ± 0.228 µm, while a fragment (heart shape) was observed in the effluent sample from the municipal wastewater treatment plant (Plant C), with a diameter of 1 351.5 ± 0.449 µm (Figs 10c and 10d). A film particle obtained from the municipal wastewater treatment plant (Plant C) influent is shown in Fig. 10e and 10f, with a diameter of 388.7 ± 0.088 µm. All identified microplastics had diameters below the 5 mm threshold, a defining characteristic of microplastics (Ilechukwu et al., 2019).

Table 1. A description of microplastics detected in the industrial water treatment plants, Plants A and B, and the municipal wastewater treatment plant, Plant C

Treatment plant	Sampling site	Shape	Colour	Type
Plants A and B (industrial water treatment plants)	Raw water	Linear	Black, red, and blue	Fibres
	Clarifier outlet	Linear	Black and red	Fibres
	Mixed bed outlet	Linear	Orange	Fibres
Plant C (municipal wastewater treatment plant)	Influent	Linear and spherical	White, green, and semi-translucent	Film, fibres
	Effluent	Linear, spherical, heart	Black, semi-translucent, orange, and silver	Fragment, glitter, film, and fibres

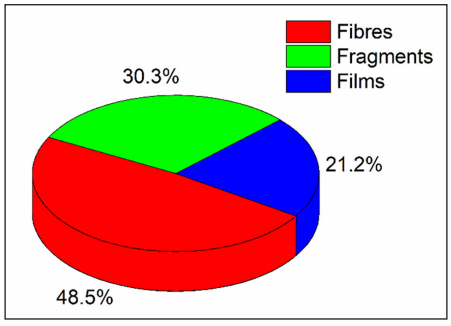

Figure 9. The types and percentage distribution of microplastics detected in industrial water treatment plants, Plants A and B, and the municipal wastewater treatment plant, Plant C

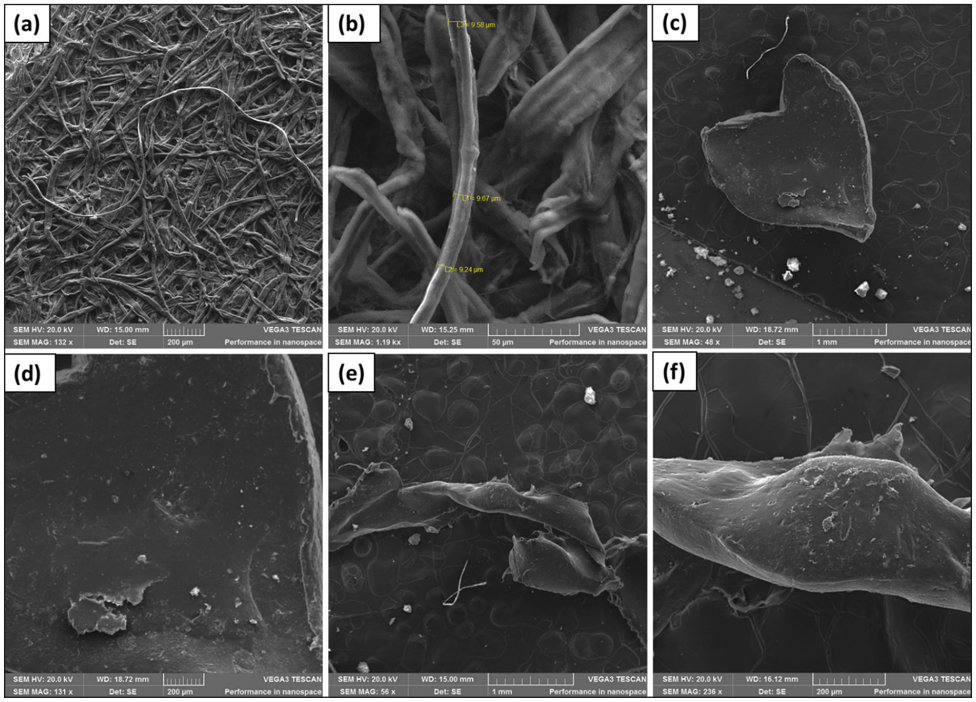

Figure 10. SEM images of microplastics: (a) fibre at low magnification, (b) fibre at high magnification, (c) fragment (heart-shaped) at low magnification, (d) fragment (heart-shaped) at high magnification, (e) film microplastic at low magnification, and (f) film microplastic at high magnification

FTIR analysis of microplastics

Figure 11 illustrates the FTIR spectra of microplastics collected from industrial water treatment plants, Plants A and B, as well as from the municipal wastewater treatment plant, Plant C. The analysis was performed on selected water samples where microplastics were visually identified and isolated. As shown in Fig. 11(a), characteristic absorption peaks were observed at 3 286 cm^{-1} (–OH stretching), 2 919 cm^{-1} and 2 851 cm^{-1} (–CH asymmetric and symmetric stretching), and 1 440 cm^{-1} (–CH bending vibration). These features are typical of polyethylene, and consistent with the findings of Athulya et al. (2023), who reported similar peaks at 3 300 cm^{-1}, 2 920 cm^{-1}, and 2 850 cm^{-1} for polyethylene-based microplastics collected from marine and freshwater ecosystems. Figure 11b showed distinct vibration peaks at 3 288 cm^{-1} (–NH stretching), 2 922 cm^{-1} (–CH stretching), and 1 639 cm^{-1} (–C=O stretching), which confirm the presence of nylon-6. These spectral features correspond well with those reported by Chen et al. (2020), Bergmann et al. (2015), and Song et al. (2015), who observed peaks at 3 300–3 270 cm^{-1} (–NH), 2 920–2 850 cm^{-1} (-CH), and 1 635–1 640 cm^{-1} (–C=O) which affirmed that the microplastics were made of nylon-6. The presence of nylon-6 is generally associated with synthetic fibres originating from textile industries and domestic laundry wastewater. The similarity of these spectral peaks suggests that the microplastics detected in this study likely share a common polymeric composition and source with those identified in previous investigations, confirming the reliability of FTIR as a diagnostic tool for polymer identification in environmental samples.

Average length of microplastics in the industrial water treatment plants, Plants A and B, and the municipal wastewater treatment plant, Plant C

The average lengths of microplastics were measured using ImageJ (Fig. 12). In the industrial water treatment plant, Plant A, the average microplastic sizes were 0.44 ± 1.87 mm, 0.70 ± 2.35 mm, and 0.95 ± 0.90 mm for raw water, clarifier outlet, and mixed bed outlet, respectively (Fig. 12a). Whilst for Plant B (industrial water treatment plant), the average lengths recorded were 0.98 ± 2.55 mm and 0.85 ± 0.38 mm for the raw water and clarifier outlet, respectively (Fig. 12b). In the municipal wastewater treatment plant, Plant C, the average microplastics length was 1.69 ± 0.25 mm in the influent and 0.81 ± 0.91 mm in the effluent (Fig. 12c).

These findings demonstrate that both industrial water treatment plants, Plants A and B, exhibit progressive removal of microplastics as water passes through the treatment stages, with larger particles being more efficiently removed during clarification. However, the residual microplastics remain detectable at later stages, particularly in the mixed bed outlet of Plant A. This can be attributed to polystyrene-based ion exchange resins, which are susceptible to shedding fragments into the treated water (Haddad et al., 2019). Similarly, the municipal wastewater treatment plant, Plant C, achieved a substantial reduction in microplastic length between influent and effluent samples, confirming the role of biological and tertiary processes in reducing microplastic contamination. Nonetheless, the persistence of small-sized microplastics in final effluents underscores the limitations of conventional treatment processes and highlights the necessity for advanced membrane or catalyst-based approaches to achieve near-complete removal.

Filtration separation performance for microplastics

Microplastics extracted only from the municipal wastewater treatment plant, Plant C, were used to investigate membrane rejection and the mechanism for this. Figure 13 shows the percentage rejection of microplastics by pristine PES and HPEI/PES membranes. The modified membranes achieved high rejection efficiencies (95.00–97.33%), significantly outperforming the pristine PES, which exhibited a rejection rate of 84.21%. The high rejection of the microplastics by the HPEI/PES membranes can be attributed to two main mechanisms: (i) hydrophilic–hydrophobic interactions and (ii) size exclusion.

The HPEI/PES membranes exhibited significantly lower contact angles (41 ± 0.066–51 ± 0.064°) compared to pristine PES (86 ± 0.057°), confirming their improved hydrophilic character (Table 2). The presence of peripheral $–NH_2$ groups in HPEI enables hydrogen bonding with water molecules, which generates a hydration layer on the membrane surface. This hydrated interface repels hydrophobic microplastics, reducing their affinity for the membrane surface and improving rejection. Similar findings have been reported by Wang et al. (2021), who investigated the influence of hydrophilic surface modifications on membrane performance and fouling resistance. In their study, polyethersulfone (PES) membranes were modified with hydrophilic functional groups such as hydroxyl (–OH), carboxyl (–COOH), and sulfonic ($–SO_3H$) groups. These modifications significantly enhanced the membranes' surface wettability and hydrophilicity, promoting the formation of a stable hydration layer at the membrane water interface. This hydration layer acts as an energetic barrier that prevents the direct adhesion of hydrophobic foulants and microplastic particles onto the membrane surface, thereby improving antifouling behaviour and rejection efficiency.

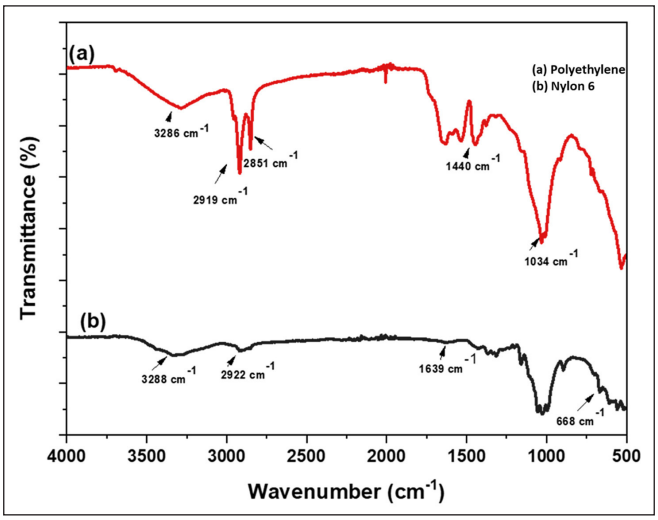

Figure 11. FTIR spectra of microplastics detected in the industrial water treatment plants, Plants A and B, and municipal wastewater treatment plant, Plant C

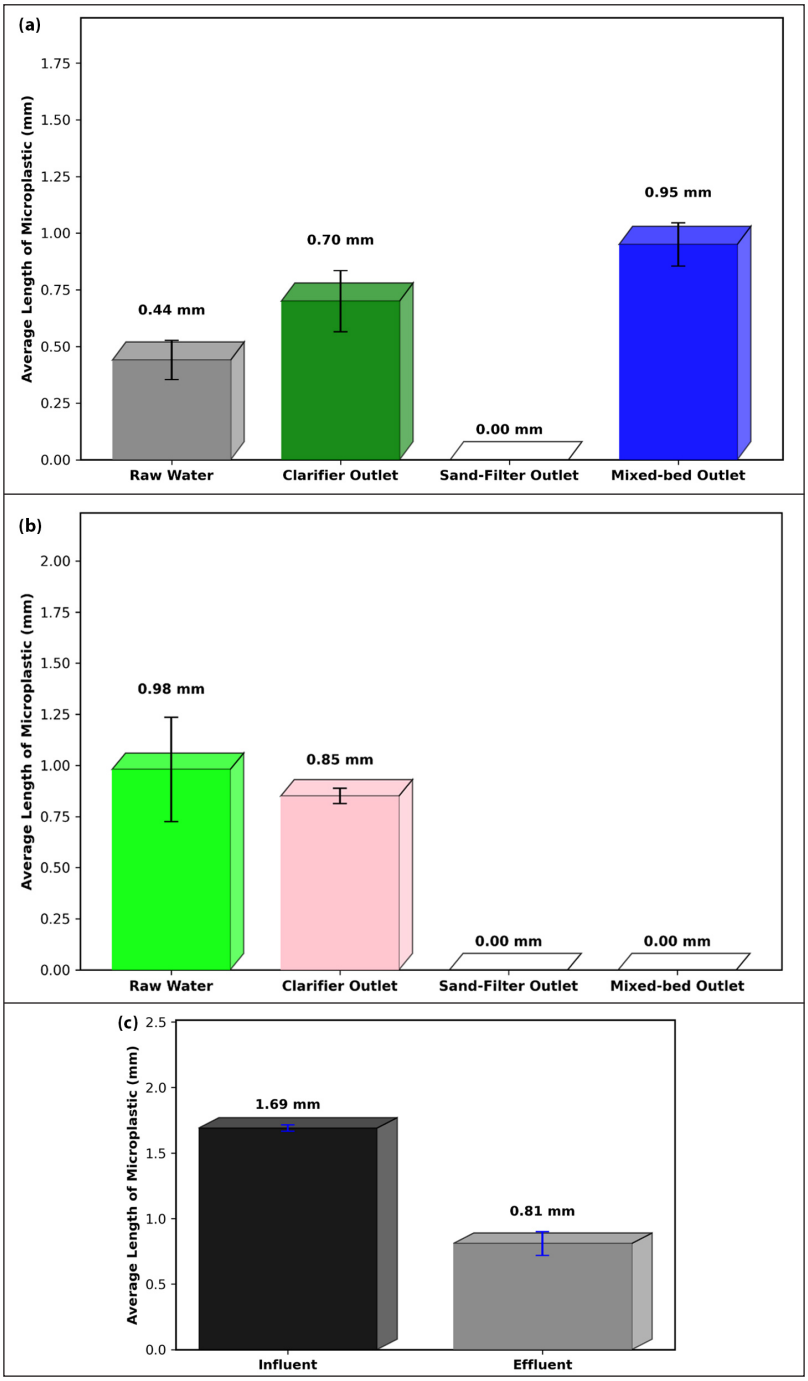

Figure 12. Average length of microplastics measured in the industrial water treatment plants: (a) Plant A and (b) Plant B, and (c) the municipal wastewater treatment plant, Plant C

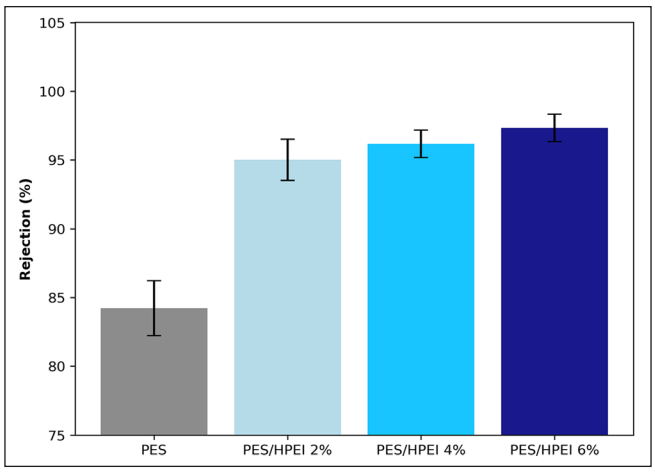

Figure 13. Percentage rejection of microplastics for pristine PES membrane and PES/HPEI membranes

Table 2. Pore size and contact angle analysis for pristine PES and HPE/PES membranes

Membrane	Pore size (µm)	Contact angle (°)
Pristine PES	0.0683 ± 0.00030	86 ± 0.057
HPEI/PES 2%	0.00373 ± 0.00003	41 ± 0.066
HPEI/PES 4%	0.00416 ± 0.00005	49 ± 0.061
HPEI/PES 6%	0.00459 ± 0.00004	51 ± 0.064

The enhanced hydration interaction also reduces Van der Waals attractions between the membrane and microplastic surfaces, facilitating easier detachment during backwashing or continuous filtration. Similar mechanisms were described by Zhang et al. (2025), who observed that introducing oxygen- and nitrogen-containing polar groups increased water affinity, decreased contact angle, and improved microplastic removal efficiency. Collectively, these studies demonstrate that surface functionalisation with hydrophilic groups not only improves antifouling resistance but also strengthens the selective hydration-repulsion mechanisms that govern microplastic rejection during membrane filtration.

Size exclusion was also identified as another key mechanism. The pristine PES membrane exhibited a pore size of 0.0683 ± 0.00030 µm, while the modified HPEI/PES membranes showed reduced pore sizes in the range 0.00373 ± 0.00003–0.00459 ± 0.00004 µm (Table 2), in line with PES-based nanofiltration membranes, which have been reported to have pore sizes of 0.001 to 0.01 µm (Covaliu-Mierlă et al., 2023). The microplastics extracted from the influent had an average of 9.50 ± 0.228 µm, which is much larger than the pores of both pristine and modified membranes. This large size differential indicates that rejection was primarily governed by steric hindrance, where particles larger than the pores are physically excluded from passing through the membrane. Molina et al. (2023) reported that microplastics slightly larger than membrane pores are fully retained, while smaller particles can pass through, consistent with the molecular sieving mechanism. The reduced pore size in HPEI/PES membranes enhanced the steric hindrance effect, while providing a greater tortuosity, further restricting microplastic particle passage.

Overall, these results confirm that both hydrophilic surface interactions and size-exclusion mechanisms contribute significantly to microplastic rejection. While pristine PES membranes were able to retain most microplastics due to their relatively small pore size compared to particle dimensions, HPEI modification further enhanced rejection performance by combining a hydration-layer repulsion effect with reduced pore size and increased surface polarity. These findings are consistent with previous literature on membranes. Madaeni and Ghaemi (2007) reported that hydrophilic modification of PES membranes enhances water flux and reduces fouling by forming a hydration barrier that limits the attachment of organic and particulate matter. Similarly, Molina et al. (2023) demonstrated that membrane systems with smaller effective pore diameters achieve higher microplastic removal efficiency through combined size-exclusion and electrostatic repulsion mechanisms.

CONCLUSION

This study demonstrated that microplastics are prevalent in both industrial water treatment plants and municipal wastewater treatment plants, with distinct variations in their morphology and sources. The industrial water treatment plants, Plants A and B, supplied by the Vaal and Usutu Rivers, respectively, were dominated by linear fibres. In contrast, the domestic wastewater treatment plant, Plant C, contained a broader range of microplastics, with transparent films and fragments being the most abundant, likely derived from industrial packaging and the breakdown of larger plastics. Quantitative analysis revealed that fibres were the most dominant category (48.5%), followed by fragments (30.3%) and films (21.2%). The dominance of fibres in all three plants is characteristic of secondary microplastics originating from textiles and related degradation processes.

The application of polyamide-modified membranes significantly enhanced microplastic removal efficiency compared to the pristine PES membrane. This improvement was attributed to increased hydrophilicity and reduced pore size, which promoted hydrophilic–hydrophobic repulsion and size exclusion mechanisms. Notably, the HPEI/PES 6% membrane achieved the highest rejection rate, of 97.33%, confirming the effectiveness of surface modification in enhancing performance. Overall, these findings highlight the critical role of membrane technology, particularly nanofiltration, as a final polishing step in wastewater treatment processes. By effectively rejecting microplastics, such membranes provide a promising solution for mitigating microplastic pollution in aquatic environments and protecting water quality for both industrial and municipal applications.

ACKNOWLEDGEMENTS

The South Africa/India Joint Science and Technology Research Collaboration (IND190911475982) and National Research Foundation-Competitive Support for Unrated Researchers (SRUG210407592746), the Centre for Nanomaterials Science (University of Johannesburg), Global Excellence Stature (4.0) (University of Johannesburg), Joint Research Centre for Water, Environmental Science Technology (University of Johannesburg), and Faculty of Science (University of Johannesburg), are all acknowledged by the authors for their support.

AUTHOR CONTRIBUTIONS

Michela K Masango: writing original draft, visualisation, methodology, investigation, sample/data analysis, interpretation of results, and conceptualisation. Nonhlangabezo Mabuba: conceptualisation and methodology of the study, interpretation of results, revision after review editing, and supervision. Gokul Sreekumar: revision after review. Praveen Keerthi: revision after review. Soraya P Malinga: supervision, resource, funding application, methodology of the study, conceptualisation and methodology of the study, editing, review and revision after review.

ORCID

Soraya P Malinga
https://orcid.org/0000-0003-0139-9781

REFERENCES

ATHULYA PA and CHANDRASEKARAN N (2023) Interactions of natural colloids with microplastics in the aquatic environment and its impact on FTIR characterization of polyethylene and polystyrene microplastics. *J. Mol. Liq.* **369** 120950. https://doi.org/10.1016/j.molliq.2022.120950

ATHIRA VB, MOHANTY S and NAYAK SK (2020) Preparation and characterization of porous polyethersulfone (PES) membranes with improved biocompatibility by blending sulfonated polyethersulfone (SPES) and cellulose acetate (CA): A comparative study. *Mater. Today Commun.* **25** 101544. https://doi.org/10.1016/j.mtcomm.2020.101544

BAYO J, OLMOS S and LÓPEZ-CASTELLANOS J (2020) Microplastics in an urban wastewater treatment plant: The influence of physicochemical parameters and environmental factors. *Chemosphere* **238** 124593. https://doi.org/10.1016/j.chemosphere.2019.124593

BERGMANN M, GUTOW L and KLAGES M (2015) *Marine Anthropogenic Litter*. Springer, Cham. 447 pp. https://doi.org/10.1007/978-3-319-16510-3

BERNARD N, METIAN M, OBERHAENSLI F, SZNAIDER F, RUBERTO L, VODOPIVEZ C, MacCORMACK W and HERNANDEZ CA (2025) Identification and quantification of microplastics in the Antarctic coastal waters using laser direct infrared (LDIR). *Mar. Pollut. Bull.* **221** 118534. https://doi.org/10.1016/j.marpolbul.2025.118534

BLACKLEDGE RD and JONES EL Jr (2007) All that glitters is gold! In: Blackledge RD (ed.) *Forensic Analysis on the Cutting Edge: New Methods for Trace Evidence Analysis*. John Wiley & Sons, Inc., Hoboken. 32 pp. https://doi.org/10.1002/9780470166932

BONTHUYS J (2018) Death in a drop: Study explores microplastic pollution. *The Water Wheel* January/February 2018. 12 URL: https://journals.co.za/doi/pdf/10.10520/EJC-c3504ac4b (Accessed 10 October 2025).

CASELLA C, SOL D, LACA A and DÍAZ M (2025) Microplastic retention in secondary sewage sludge: characterization and influence of solid concentration. *Appl. Sci.* **15** (7) 3557. https://doi.org/10.3390/app15073557

CHEN Y, WEN D, PEI J, FEI Y, OUYANG D, ZHANG H and LUO Y (2020) Identification and quantification of microplastics using Fourier-transform infrared spectroscopy: Current status and future prospects. *Curr. Opin. Environ. Sci. Health* **18** 1814–1819. https://doi.org/10.1016/j.coesh.2020.05.004

COVALIU-MIERLĂ CI, PĂUNESCU O and IOVU H (2023) Recent advances in membranes used for nanofiltration to remove heavy metals from wastewater: a review. *Membranes* **13** (7) 643. https://doi.org/10.3390/membranes13070643.

DEY TK, UDDIN ME and JAMAL M (2021) Detection and removal of microplastics in wastewater: evolution and impact. *Environ. Sci. Pollut. Res.* **28** (14) 16925–16947. https://doi.org/10.1007/s11356-021-12943-5

DEVRIESE LI, VAN DER MEULEN MD, MAES T, BEKAERT K, PAUL-PONT I, FRÈRE L and VETHAAK AD (2015) Microplastic contamination in brown shrimp (*Crangon crangon*, Linnaeus 1758) from coastal waters of the Southern North Sea and Channel area. *Mar. Pollut. Bull.* **98** (1–2) 179–187. https://doi.org/10.1016/j.marpolbul.2015.06.051

ENFRIN M, LEE J, LE-CLECH P and DUMEE LF (2020) Kinetic and mechanistic aspects of ultrafiltration membrane fouling by nano- and microplastics. *J. Membr. Sci.* **601** 117890. https://doi.org/10.1016/j.memsci.2020.117890

FUSCHI C, PU H, MACDONELL M, PICEL K, NEGRI M and CHEN J (2022) Microplastics in the Great Lakes: Environmental, health, and socioeconomic implications and future directions. *ACS Sustain. Chem. Eng.* **10** (43) 14074–14091. https://doi.org/10.1021/acssuschemeng.2c02896

GYEDU-ABABIO T and VAN WYK F (2004) Effects of human activities on the Waterval River, Vaal River catchment, South Africa. *Afr. J. Aquat. Sci.* **29** (1) 75–81. https://doi.org/10.2989/16085910409503794

HADDAD M, OIE C, DUY SV, SAUVÉ S and BARBEAU B (2019) Adsorption of micropollutants present in surface waters onto polymeric resins: Impact of resin type and water matrix on performance. *Sci. Total Environ.* **660** 1449–1458. https://doi.org/10.1016/j.scitotenv.2018.12.247

HIDAYATURRAHMAN H and LEE TG (2019) A study on characteristics of microplastic in wastewater of South Korea: Identification, quantification, and fate of microplastics during treatment process. *Mar. Pollut. Bull.* **146** 696–702. https://doi.org/10.1016/j.marpolbul.2019.06.071

HORTON AA, JÜRGENS MD, LAHIVE E, VAN BODEGOM PM and VIJVER MG (2018) The influence of exposure and physiology on microplastic ingestion by the freshwater fish *Rutilus rutilus* (roach) in the River Thames, UK. *Environ. Pollut.* **236** 188–194. https://doi.org/10.1016/j.envpol.2018.01.044

ILECHUKWU I, NDUKWE GI, MGBEMENA NM and AKANDU AU (2019) Occurrence of microplastics in surface sediments of beaches in Lagos, Nigeria. *Eur. Chem. Bull.* **8** (11) 371–375.

ILECHUKWU I, FOURREAU CJL, STOELTJE M, CONN E, IWAKI Y and REIMER JD (2025) Abundance and distribution of microplastics on sandy beaches of remote islands of Okinawa, southern Japan. *Estuar. Coast. Shelf Sci.* **326** 109538. https://doi.org/10.1016/j.ecss.2025.109538

JIANG Q, NGO HH, NGHIEM LD, HAI FI, PRICE WE, ZHANG J, LIANG S, DENG L and GUO W (2018) Effect of hydraulic retention time on the performance of a hybrid moving bed biofilm reactor-membrane bioreactor system for micropollutants removal from municipal wastewater. *Bioresour. Technol.* **247** 1228–1232. https://doi.org/10.1016/j.biortech.2017.09.114

JUIZO D and HJORTH P (2009) Application of a district management approach to Southern African river basin systems: The case of the Umbeluzi, Incomati and Maputo river basins. *Water Policy* **11** (6) 719–730. https://doi.org/10.2166/wp.2009.301

LAFORCE E, CORNELISSEN ER, VERMEIR P and DE CLERCQ J (2025) Insights into biopolymer and humics natural organic matter removal mechanisms by anion exchange resins. *Water Pract. Technol.* **20** (4) 826–839. https://doi.org/10.2166/wpt.2025.048

LETSWALO VP, DLAMINI LN and MALINGA SP (2022) Efficient degradation of tetracycline using a nanostructured g-C_3N_4/Nb_2O_5/HPEI/PES photocatalytic membrane. *Environ. Adv.* **10** 100322. https://doi.org/10.1016/j.envadv.2022.100322

LIAO C, ZHAO J, YU P, TONG H and LUO Y (2012) Synthesis and characterization of low content of different SiO_2 materials composite poly (vinylidene fluoride) ultrafiltration membranes. *Desalination* **285** 117–122. https://doi.org/10.1016/j.desal.2011.09.042

LONG Z, PAN Z, WANG W, REN J, YU X, LIN L, LIN H, CHEN H and JIN X (2019) Microplastic abundance, characteristics, and removal in wastewater treatment plants in a coastal city of China. *Water Res.* **155** 255–265. https://doi.org/10.1016/j.watres.2019.02.028

MA B, XUE W, DING Y, HU C, LIU H and QU J (2019a) Removal characteristics of microplastics by Fe-based coagulants during drinking water treatment. *J. Environ. Sci.* **78** 267–275. https://doi.org/10.1016/j.jes.2018.10.006

MA B, XUE W, HU C, LIU H, QU J and LI L (2019b) Characteristics of microplastic removal via coagulation and ultrafiltration during drinking water treatment. *Chem. Eng. J.* **359** 159–167. https://doi.org/10.1016/j.cej.2018.11.155

MADAENI SS and GHAEMI N (2007) Characterization of self-cleaning RO membranes coated with TiO_2 particles under UV irradiation. *J. Membr. Sci.* **303** (1–2) 221–233. https://doi.org/10.1016/j.memsci.2007.07.017

MOLINA S, OCAÑA-BIEDMA H, RODRÍGUEZ-SÁEZ L and LANDABURU-AGUIRRE J (2023) Experimental evaluation of the process performance of MF and UF membranes for the removal of nanoplastics. *Membranes* **13** (7) 683. https://doi.org/10.3390/membranes13070683

MULLER A, WENTZEL M, SAAYMAN G, VAN DER MERWE S, ESTERHUYSE C, SNYMAN J and EKAMA G (2004) Full-scale implementation of external nitrification biological nutrient removal at the Daspoort Wastewater Treatment Works. *Water SA* **30** (5) 37–43. https://doi.org/10.4314/wsa.v30i5.5164

NAJI A, NURI M and VETHAAK AD (2018) Microplastics contamination in molluscs from the northern part of the Persian Gulf. *Environ. Pollut.* **235** 113–120. https://doi.org/10.1016/j.envpol.2017.12.046

NKOSI SD, MALINGA SP and MABUBA N (2022) Microplastics and heavy metals removal from freshwater and wastewater systems using a membrane. *Separations* **9** (7) 166. https://doi.org/10.3390/separations9070166

NOURI M, MASSAHI T and HOSSINI H (2025) Microplastics in human body: a narrative on routes of exposure to contamination and potential health effects. *Environ. Pollut. Bioavail.* **37** (1) 2538535. https://doi.org/10.1080/26395940.2025.2538535

PILEVAR Z, BAHRAMI A, BEIKZADEH S, HOSSEINI H and JAFARI SM (2019) Migration of styrene monomer from polystyrene packaging materials into foods: Characterization and safety evaluation. *Trends Food Sci. Technol.* **91** 248–261. https://doi.org/10.1016/j.tifs.2019.07.020

POERIO T, LAVORATO C, SEVERINO A, RUSSO B, MOLINARI R, ARGURIO P and FIGOLI A (2024) Combined membrane separation and photocatalysis process for the recovery and decomposition of micro/nanoplastics from polyester fabrics. *J. Environ. Chem. Eng.* **12** (5) 113310. https://doi.org/10.1016/j.jece.2024.113310.

PRATA JC, REIS V, DA COSTA JP, MOUNEYRAC C, DUARTE AC and ROCHA-SANTOS T (2021) Contamination issues as a challenge in quality control and quality assurance in microplastics analytics. *J. Hazardous Mater.* **403** 123660. https://doi.org/10.1016/j.jhazmat.2020.123660

RUSSO, B, LAVORATO C, ARGURIO P, LIMONTI C, SICILIANO A, FIGOLI A and POERIO T (2025) Nanofiltration as an effective tertiary treatment for the removal of micro- and nanoplastics from municipal water effluent. *Sep. Purif. Technol.* **376** 3 1383–5866. https://doi.org/10.1016/j.seppur.2025.134121

SONG YK, HONG SH, JANG M, HAN GM, RANI M, LEE J and SHIM WJ (2015) A comparison of microscopic and spectroscopic identification methods for analysis of microplastics in environmental samples. *Mar. Pollut. Bull.* **93** (1–2) 202–209. https://doi.org/10.1016/j.marpolbul.2015.01.015

VLOTMAN DE, NGILA JC, NDLOVU T and MALINGA SP (2018) Hyperbranched polymer integrated membrane for the removal of arsenic(III) in water. *J. Membr. Sci. Res.* **4** (2) 53–62. https://doi.org/10.22079/jmsr.2017.67560.1148

WANG Z, SEDIGHI M and LEA-LANGTON A (2020) Filtration of microplastic spheres by biochar: removal efficiency and immobilisation mechanisms. *Water Res.* **184** 116165. https://doi.org/10.1016/j.watres.2020.116165

WEPENER VV, VAN DYK C, BERVOETS L, O'BRIEN G, COVACI A and CLOETE Y (2011) An assessment of the influence of multiple stressors on the Vaal River, South Africa. *Phys. Chem. Earth A/B/C* **36** (14–15) 949–962. https://doi.org/10.1016/j.pce.2011.07.075

ZHANG J, DING W, ZOU G, WANG X, ZHAO M, GUO S and CHEN Y (2023) Urban pipeline rainwater runoff is an important pathway for land-based microplastics transport to inland surface water: A case study in Beijing. *Sci. Total Environ.* **861** 160619. https://doi.org/10.1016/j.scitotenv.2022.160619

ZHANG S, YANG X, GERTSEN H, PETERS P, SALÁNKI T and GEISSEN V (2018) A simple method for the extraction and identification of light density microplastics from soil. *Sci. Total Environ.* **616** 1056–1065. https://doi.org/10.1016/j.scitotenv.2017.10.213

ZHANG H, WANG T, FAN L, LIU X, DONG Y, CHEN M, WANG Y, ZHANG Q and ZOU Y (2024) Quaternization cross-linking of hyperbranched polyethylene-graft-poly(diethylaminoethyl methacrylate) as antimicrobial separation layer of molecular sieving membrane. *J. Membr. Sci.* **692** 122313. https://doi.org/10.1016/j.memsci.2023.122313

ZHENG Y, ZHU J, LI J, LI G and SHI H (2023) Burrowing invertebrates induce fragmentation of mariculture Styrofoam floats and formation of microplastics. *J. Hazardous Mater.* **447** 130764. https://doi.org/10.1016/j.jhazmat.2023.130764

APPENDIX

Preparation of HPEI/PES membranes

The membranes were prepared following a method adapted from Vlotman et al. (2018). Briefly, branched polyethyleneimine (HPEI) was dissolved in a 90:10 (v/v) water–ethanol mixture to prepare aqueous solutions containing 2%, 4%, and 6% (w/v) HPEI. The commercial PES membranes were then immersed in these solutions for 6 h at room temperature, allowing for surface adsorption and diffusion of the polymer. Subsequently, the membranes were dipped into a 0.1% (w/v) solution of trimesoyl chloride (TMC) in n-hexane for 60 s to initiate interfacial crosslinking. To promote further crosslinking and solvent removal, the membranes were dried at 60 °C for 10 min and then rinsed with n-hexane to eliminate any unreacted TMC residues.

Table A1. Composition of pristine and HPEI-modified PES membranes

Membrane type	HPEI concentration (% w/v)	HPEI mass (g)	Solvent composition (water/ethanol)	TMC concentration (% w/v)	TMC mass (g)
Pristine PES	0	—	—	—	—
HPEI/PES-2%	2	2.0	90/10	0.1	0.1
HPEI/PES-4%	4	4.0	90/10	0.1	0.1
HPEI/PES-6%	6	6.0	90/10	0.1	0.1

Table A2. Porosity and membrane thickness

Membrane	Water uptake (%)	Porosity (%)	Thickness (μm)	Pore size (μm)	Contact angle (°)	W_d (g) / W_w (g)
Pristine PES	49.02	57.93	145	0.06830 ± 0.00030	86 ± 0.057	0.01714 / 0.02554
HPEI/PES 2%	72.33	47.53	162	0.00373 ± 0.00003	41 ± 0.066	0.01065 / 0.01835
HPEI/PES 4%	79.71	36.12	212	0.00416 ± 0.00005	49 ± 0.061	0.00961 / 0.01726
HPEI/PES 6%	84.15	44.72	246	0.00459 ± 0.00004	51 ± 0.064	0.01307 / 0.02407